

Annealing-insensitive “black silicon” with high infrared absorption

Yan Peng, Xiangqian Chen, Yunyan Zhou, Gongjie Xu, Bin Cai, Yiming Zhu, Jian Xu, Ron Henderson, and Jianming Dai

Citation: *Journal of Applied Physics* **116**, 073102 (2014); doi: 10.1063/1.4893584

View online: <http://dx.doi.org/10.1063/1.4893584>

View Table of Contents: <http://scitation.aip.org/content/aip/journal/jap/116/7?ver=pdfcov>

Published by the [AIP Publishing](#)

Articles you may be interested in

[Crystalline silicon growth in nickel/a-silicon bilayer](#)

AIP Conf. Proc. **1512**, 686 (2013); 10.1063/1.4791223

[Defect engineering of the oxygen-vacancy clusters formation in electron irradiated silicon by isovalent doping: An infrared perspective](#)

J. Appl. Phys. **112**, 123517 (2012); 10.1063/1.4770488

[Optical constants of silicon in near infrared region](#)

Appl. Phys. Lett. **93**, 131916 (2008); 10.1063/1.2994669

[Analysis of native oxide growth process on an atomically flattened and hydrogen terminated Si \(111\) surface in pure water using Fourier transformed infrared reflection absorption spectroscopy](#)

J. Vac. Sci. Technol. A **16**, 375 (1998); 10.1116/1.581008

[Photoelectron and infrared spectroscopy of semi-insulating silicon layers](#)

J. Appl. Phys. **82**, 3519 (1997); 10.1063/1.365670



AIP | Journal of Applied Physics

Journal of Applied Physics is pleased to announce **André Anders** as its new Editor-in-Chief

Annealing-insensitive “black silicon” with high infrared absorption

Yan Peng,^{1,2,a)} Xiangqian Chen,¹ Yunyan Zhou,¹ Gongjie Xu,¹ Bin Cai,¹ Yiming Zhu,^{1,b)} Jian Xu,³ Ron Henderson,⁴ and Jianming Dai²

¹Shanghai Key Laboratory of Modern Optical System, Engineering Research Center of Optical Instrument and System Ministry of Education, University of Shanghai for Science and Technology, Shanghai 200093, China

²The Institute of Optics, University of Rochester, Rochester, New York 14627, USA

³Department of Engineering Science and Mechanics, The Pennsylvania State University, University Park, Pennsylvania 16802, USA

⁴Department of Physics & Astronomy, Middle Tennessee State University, Murfreesboro, Tennessee 37132, USA

(Received 25 June 2014; accepted 9 August 2014; published online 21 August 2014)

A black silicon structure with high-aspect-ratio surface spikes was designed and fabricated in vacuum, resulting in absorptance $>90\%$ over the range of 200–2500 nm. It is demonstrated that annealing, an essential step in the fabrication of semiconductor devices, has almost no effect on the infrared absorption of this material, while the infrared absorption of an identical structure fabricated in a SF₆ drops dramatically after the annealing process. The characteristic of high infrared absorption and annealing-insensitivity is attributed to both the high-aspect-ratio structure and the phosphor-doped low impedance silicon. These results are important for the fabrication of highly efficient optoelectronic devices. © 2014 AIP Publishing LLC.

[<http://dx.doi.org/10.1063/1.4893584>]

I. INTRODUCTION

Silicon is one of the most popular materials in semiconductor devices for its wide array of applications in solar energy cells and optoelectronic detectors. However, the band gap of 1.1 eV limits applications in the infrared region of the spectrum. Since black silicon fabricated by femtosecond laser pulses was first reported by Mazur *et al.*,¹ the near-unity high infrared absorption of this novel microstructure has attracted more and more interest.^{2–5} For this kind of materials, light absorption in the infrared range ($>0.8\ \mu\text{m}$) can be enhanced beyond 90%, which increases the potential applications in silicon-based photovoltaic,^{6,7} photo-detectors,^{8,9} terahertz emitter,^{10,11} and super-hydrophobic devices.^{12,13} Usually, these silicon microstructures are fabricated in an ambient of sulfur-bearing gases, such as SF₆ and H₂S,^{2,14} where the impurity sulfur atoms can concentrate within the microstructure surfaces during the spike formation process, resulting in an increased absorptance in the infrared region. However, the sulfur-incorporated material lost its ability of broadband optical absorption under the high temperatures associated with ohmic contact formation and passivation processes, which are necessary during the manufacture of infrared sensors. As a result, the high absorption in the infrared region decreases dramatically. For example, for a silicon wafer [n-Si (111), 260 μm thick, with resistivity $\rho = 8\text{--}12\ \Omega\ \text{m}$] irradiated by a train of 800 nm, 100 fs laser pulses in the presence of SF₆ gas, the absorptance of the microstructured silicon at 1550 nm can be as high as 90%, but drops to 40% after a 500 °C annealing process.¹⁵ Another disadvantage of using sulfur-containing gases is that, after high temperature processes, the sulfur

impurities in the bulk silicon often become inactivated states, which act as recombination centers that can capture photo-excited carriers and greatly decrease device photocurrents. Decrease in the post-annealing absorptance and device photocurrent greatly reduces the efficiency of optoelectronic devices that employ black silicon.

On the other side, if black silicon are fabricated directly in the vacuum, the surface microstructure can only decrease the reflectance of material in the visible region, but has no contribution to the infrared absorption.¹⁶ Therefore, dopant impurities are necessary for the improvement of infrared absorption.

Other dopant impurities in the silicon substrate (such as phosphor or arsenic) also contribute to the infrared absorption of the material. However, the contributions are usually of such insignificance that they normally can be neglected. Kim *et al.* proved that for unstructured silicon, the infrared absorptance of sulfur-doped material can be ~ 4 times greater than that of structures doped with phosphor.¹⁷ But more importantly, the phosphor impurity in the substrate manifests as substitutional defects, which will not be affected by high temperature processing and will remain in an active state.

Based on these factors, we propose to fabricate high-aspect-ratio spike structures on phosphor-doped silicon such that incident light can experience multiple reflections (MR) between the spikes. Each reflection of light on a spike means additional opportunities to be absorbed by the phosphor impurities, leading to an increased absorption efficiency. In addition, the geometric shape of conical spikes is not significantly altered during high temperature processing. Therefore, we expect that higher spike heights are beneficial for improving the number of reflections and hence obtaining higher infrared absorptance.

In this paper, we design geometric parameters for a high-aspect-ratio spike structure, and theoretically

^{a)}Electronic mail: py@usst.edu.cn.

^{b)}Electronic mail: ymzhu@usst.edu.cn.

demonstrate the possibility of absorption enhancement resulting from the MR structure. Then, we fabricate this “black silicon” material, and experimentally show that the infrared absorptance is not only increased, but remains steady (>90%) even after high temperature annealing.

II. THEORY

To design a high-aspect-ratio spike structure with goal of absorption enhancement, the reflectance and transmittance of a single crystal silicon substrate should be considered first. For a single crystal silicon wafer, multiple reflections occur between the front and back interfaces when light is incident. Then, the total reflectance coefficient R_Σ and transmission coefficient T_Σ are calculated to be¹⁸

$$R_\Sigma = R \left[1 + \frac{(1-R)^2 \exp(-2\alpha l)}{1-R^2 \exp(-2\alpha l)} \right], \quad (1)$$

$$T_\Sigma = \frac{(1-R)^2 \exp(-\alpha l)}{1-R^2 \exp(-2\alpha l)}, \quad (2)$$

where $R = \frac{(1-n)^2+k^2}{(1+n)^2+k^2}$ is the reflection at normal incidence, n and k are the real part and the imaginary part of refractive index \tilde{n} ($\tilde{n} = n + ik$), and α and l are the absorption coefficient and thickness of the material, respectively.¹⁹ Considering that the silicon wafers used in our experiments are phosphor doped, the absorption coefficient α is calculated from the experimentally measured reflectance R_e and transmittance T_e using $\alpha = \frac{1}{l} \ln[(1-R_e)/T_e]$. For the case of the MR structure, the reflectance coefficient R_p and transmission coefficient T_p (for p-polarized light) can be calculated according to the Fresnel formulae as follows:

$$R_p = \frac{n_2 \cos \theta_1 - n_1 \cos \theta_2}{n_2 \cos \theta_1 + n_1 \cos \theta_2}, \quad (3)$$

$$T_p = \frac{2n_1 \cos \theta_1}{n_2 \cos \theta_1 + n_1 \cos \theta_2}, \quad (4)$$

where θ_1 and θ_2 are the angle of incidence and refraction, respectively; n_1 and n_2 are the refractive indices of air and silicon, respectively, where $n_1 = 1$, $n_2 = \tilde{n}$. In the model, the different geometric parameters of the spike structure will change θ_1 and θ_2 for each reflection, and thus alter R_p and T_p as well. After multiple reflections, the last R_p is considered

the final reflectance coefficient, while the final transmission coefficient is the sum of each T_p .

III. RESULT AND DISCUSSION

The resulting design is shown in Fig. 1(a). It consists of multiple conical spikes, each of whose geometric parameters include height h and base diameter d . To simplify the calculation, the surfaces of each spike were considered as smooth. Considering the non-uniform profile of the laser energy used during the fabrication process and the resulting growth characteristics of the spikes, the height and diameter parameters are designed in a range of sizes with certain proportional relations. Multiple parameter sets were examined; for example, with $h = 5-8 \mu\text{m}$, and $d = 3-5 \mu\text{m}$ the absorptance calculated at 2000 nm is $\sim 87\%$, while with $h = 15-21 \mu\text{m}$, and $d = 8-13 \mu\text{m}$ the absorptance at 2000 nm is $\sim 89\%$. The corresponding simulation results are presented in Fig. 1(b). Our model shows that when the height of the spike structure is increased by $\sim 10 \mu\text{m}$, the corresponding absorptance experiences an enhancement of about 2%. These results demonstrate that the absorptance of a high-aspect-ratio silicon spike structure is indeed greatly enhanced by the MR effect.

Based on the theoretical model, we experimentally fabricated two-dimensional high-aspect-ratio micro-spike structures on a silicon surface. The laser pulses used in the experiment were produced by a Ti:Sapphire regenerative amplifier, typically 800 nm, 1 kHz, and 130 fs. The laser beam was focused with a convex lens ($f = 1 \text{ m}$), and delivered into a chamber through a quartz window of 0.4 mm thickness. The silicon wafer (phosphor-doped n-type silicon wafer, resistivity: 0.01–0.02 $\Omega \text{ cm}$) was mounted in the vacuum chamber with the (100) face placed vertically and directed toward the laser. The laser spot on the sample surface was monitored by a CCD beam profiler (WinCamD-UCD12) and the diameter of each spot was set to about 300 μm by adjusting the distance between the silicon wafer and the laser focal point. The contrastive ambient atmospheres chosen here were SF_6 and vacuum. In order to avoid the effect of residual impurities from the ambient gas, two separate chambers were used for the microstructures fabrication, one for the SF_6 atmosphere and the other for vacuum. The pressure in the vacuum chamber was kept at $\sim 10^{-4}$ Torr constantly, while for the chamber with SF_6 , the base pressure was $\sim 10^{-4}$ Torr and then filled back with SF_6 to a pressure of 500 Torr. The chambers were mounted on motor-driven

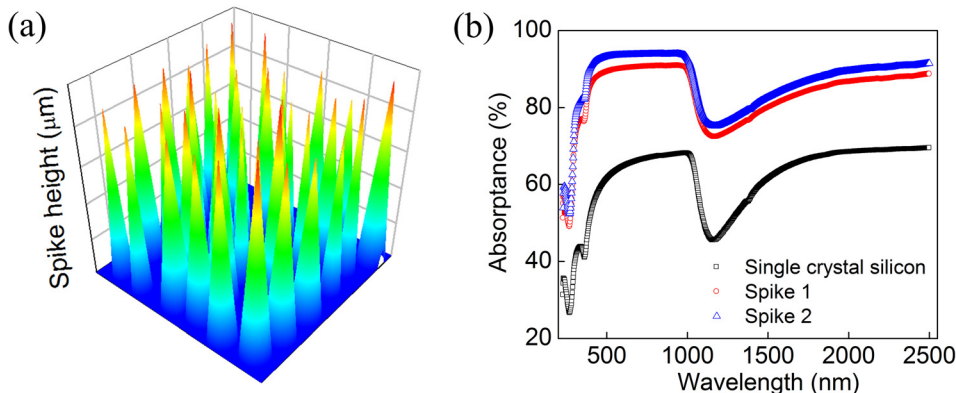


FIG. 1. (a) The proposed high-aspect-ratio spike structure. (b) Simulated absorptance of single crystal silicon and micro-spike structured silicon with different geometric parameters. For spike 1: $h = 5-8 \mu\text{m}$, $d = 3-5 \mu\text{m}$; spike 2: $h = 15-21 \mu\text{m}$, $d = 8-13 \mu\text{m}$.

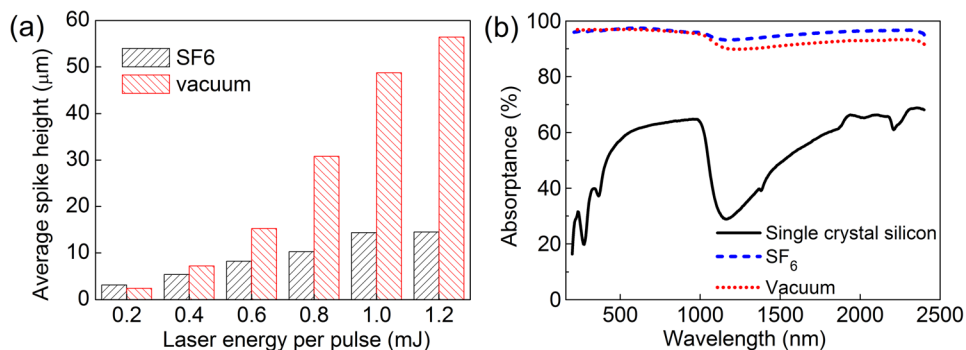


FIG. 2. (a) The average spike height of microstructures fabricated in SF₆ and vacuum as a function of laser energy per pulse. (b) The absorbance of a single crystal silicon and microstructured silicon substrates fabricated in the ambient of SF₆ and vacuum with different laser energy per pulse (1.0 mJ for SF₆ and 1.2 mJ for vacuum).

translation stages to realize two-dimensional microstructures fabrication.²⁰ According to the equation of $N = a^2 f / (VD)$,²¹ the number of shots (N) received anywhere on the sample surface (except on the edges) was 1000 (in our experiments, scanning width $a = 300 \mu\text{m}$, with laser repetition $f = 1 \text{ kHz}$, speed-velocity $V = 1200 \mu\text{m/s}$, and shift between two adjacent parallel scans $D = 75 \mu\text{m}$). Furthermore, a quarter-wave plate and polarizing beam splitter were used to adjust the intensity of the incident laser beam. The pulse number was controlled by a beam shutter (SH05, Thorlabs). The measurement of spike height was done by the scanning electron microscope (SEM). After reading a distance estimated from SEM picture, a factor of $\sqrt{2}$ is multiplied to the value because the sample is tilted 45° angle for the measurement. Each value is the average result of 5 spike heights, respectively, at each corresponding laser energy, and the measuring error is $\sim 1 \mu\text{m}$. The absorbance measurements were performed by an UV/Vis/NIR spectrometer (Lambda 1050, PerkinElmer) equipped with an integral spherical detector that integrates all transmitted or reflected light. The sample absorbance (A) is determined by the equation $A = 1 - R - T$, where T is the transmittance and R is the reflectance.

Because sulfur impurities introduced during fabrication can induce additional absorption of the microstructures, samples with the same spike height under the conditions of

vacuum and SF₆ would not be expected to exhibit the same absorbance. To clearly distinguish the absorbance changes due only to the process of annealing, it was necessary to produce samples with similar absorbance values before subjecting them to any thermal processing. Therefore, the spike heights were optimized under the condition of vacuum and SF₆ by using different laser energies (the highest laser energy we used is lower than the saturated energy permitted by the irradiated pulse number),^{22,23} i.e., the spike height was increased in the case of vacuum in order to realize a similar light absorbance (>90%) as samples fabricated in the SF₆ ambient.

The processing results shown in Fig. 2(a) clearly indicate that in the presence of SF₆, the average spike height increases from ~ 3 to $14 \mu\text{m}$ as the laser energy per pulse is raised from 0.2 to 1.0 mJ. While in the case of vacuum, the average spike height reached $56 \mu\text{m}$ with a laser energy of 1.2 mJ. The corresponding SEM pictures are partly shown in Fig. 3. After comparison, we can see that the spikes fabricated in the vacuum have less micro/nano-particles on the surface,²³ which is also beneficial for the later output of photocurrent.

The sample fabricated in SF₆ with the average spike height of $14 \mu\text{m}$ and the sample fabricated in vacuum with an average spike height of $56 \mu\text{m}$ were chosen for the light

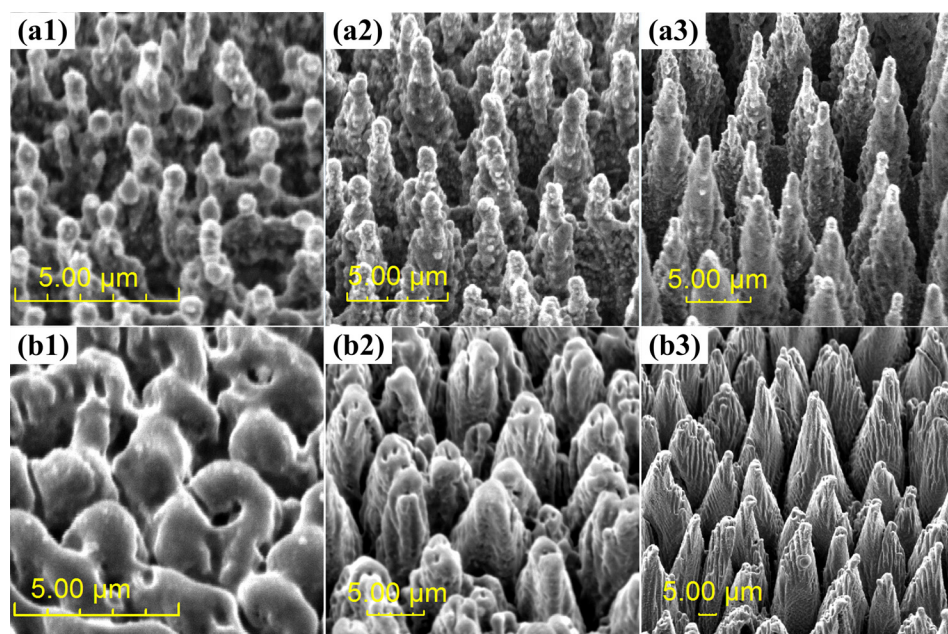


FIG. 3. SEM images of a silicon surface fabricated in the ambient of (a) SF₆, (b) vacuum. The corresponding laser energies are (a1) and (b1) 0.2 mJ, (a2) and (b2) 0.6 mJ, (a3) and (b3) 1.2 mJ, respectively. Each SEM image is taken at a 45° angle to the surface.

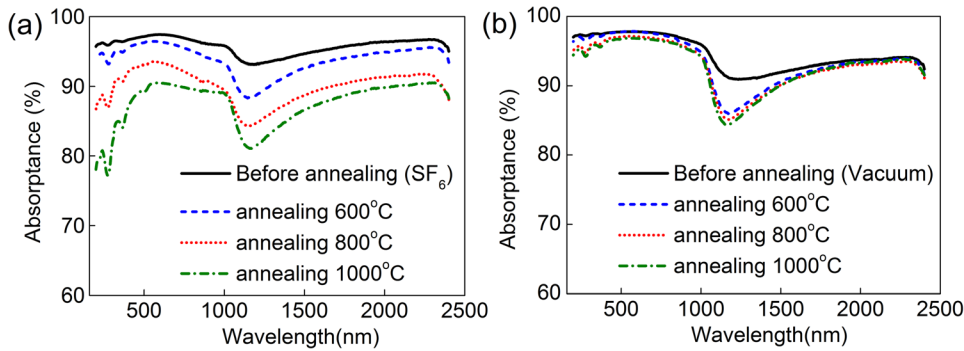


FIG. 4. The absorbance of microstructured silicon fabricated in the ambient of (a) SF_6 , (b) vacuum before and after annealing. The corresponding annealing temperatures are labeled on the figures.

absorbance measurements. The corresponding absorbance spectra shown in Fig. 2(b) demonstrate that the absorbance of both the SF_6 - and vacuum-fabricated samples remain above 90% across the spectral range being studied, and that the absorbance values of the two samples stay within 5% of each other at all wavelengths.

We believe that the difference in spike height between the SF_6 and vacuum ambient fabricated samples has two primary causes: first, the better heat-insulating property of vacuum keeps energy concentrated inside the bulk silicon; second, part of the energy is lost in the ionization process of the SF_6 gas. Under laser irradiation, the silicon wafer absorbs pulse energy. When a sufficient amount of energy is absorbed, the melting and ablative temperature of silicon is reached and an evolution that begins with capillary waves and ripples forms a quasi-periodic array of beads that leads to the formation of conical spikes on the silicon surface.²⁴ As the irradiated energy is not exceed the saturated energy permitted by the pulse number,²² the higher the temperature inside the silicon which results in more silicon material being melted and ablated. Thus, the resulting spike heights increase. In the gas ambient of SF_6 , however, the gas medium absorbs part of the laser energy and dissociates into F ions, which can facilitate a chemical reaction between silicon and SF_6 . The higher the laser energy, the more SF_6 molecules are ionized, while in the case of vacuum all the laser energy is absorbed by the substrate. Furthermore, the better heat-insulating properties of vacuum lead to more of the energy remaining within the bulk silicon, which can facilitate a further increase in spike height.

Samples were then furnace annealed in an atmosphere of flowing argon for 5 min at 600°C–800°C and 1000°C, respectively. The temperature change rate was 100°C/s (AccuThermo AW610, Rapid Thermal Process System). Figure 4 shows that before annealing, the absorbance of samples fabricated in both the SF_6 and vacuum ambient remains above 90%. After annealing, the absorbance of SF_6 samples decreases markedly, while the absorbance of the vacuum samples experiences little change except for a small range around 1100 nm.

In order to understand the different reactions of the SF_6 and vacuum prepared microstructured silicon to annealing, the factors that contribute to the high infrared absorbance of the so-called black silicon need to be identified. First, there is the formation of energy levels caused by impurity doping during the laser fabrication process. An impurity, such as sulfur, can be embedded into the microstructure surface layer during the interaction process between laser and ambient SF_6

gas. The formation of a band of sulfur impurity states overlaps the silicon band edge, thereby reducing the band gap from 1.1 eV to approximately 0.4 eV, and promoting light absorbance.¹⁵ Second, the absorption is enhanced by the MR structure. The single crystal silicon wafer used in our experiments is a low-impedance sample (0.01–0.02 Ω cm, with corresponding phosphor dopant density $\sim 10^{18} \text{ cm}^{-3}$). Usually, the contribution to the infrared absorption from phosphor impurities in the silicon wafer is limited. However, when the conical spikes are formed on the silicon surface, light can be reflected many times between these spikes. Each reflection provides another opportunity for part of the incident/reflected light to be refracted into the material and absorbed by the phosphor impurities. When these small absorption contributions are accumulated over many reflections, the infrared absorption is great improved. Therefore, for the microstructured silicon fabricated in vacuum, there are two contributions to absorption, the MR structure and phosphor impurity states, while in the case of SF_6 there are three contributions, sulfur impurity states, the MR structure, and phosphor impurity states.

Under the high temperatures associated with thermal annealing, isolated substitutional sulfur impurities (optically active state) in the bulk silicon are transformed into sulfur dimer/complex impurities (inactive states), which decrease their contribution to light absorption. Conversely, phosphor impurities in the initial silicon wafer act as stable substitutional impurities, which are always active states even at high temperature. We experimentally determined that the absorption properties of the phosphor-doped single crystal silicon did not change appreciably during the process of thermal annealing (Fig. 5). The geometric parameters of the spikes,

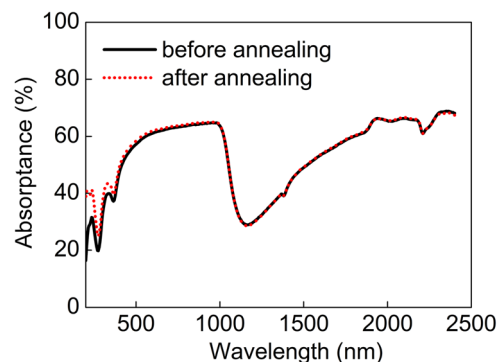


FIG. 5. The absorbance of phosphor-doped single crystal silicon before (solid line) and after annealing (dotted line).

which produce MR condition, are not affected by annealing. Therefore, the observed baseline absorption reduction in the case of SF₆ seen in Fig. 4(a) over the entire light range of 200–2500 nm can be attributed to the changes in the sulfur impurity states.

The absorption decrease around 1100 nm observed in both samples is theorized to be caused by the crystallization change in the microstructures during the process of annealing.¹⁵ The energy gap of single crystal silicon is 1.1 eV; therefore, only incident photons with wavelengths below 1100 nm can be effectively absorbed to create free carriers. When microstructures are fabricated on the silicon surface, the MR structure process enhances the infrared absorption with the help of phosphor impurities. In addition to the spiked structures, however, amorphous silicon can be formed and cover the surfaces of the spikes, which then forms a band-tail state that contributes to infrared absorption.^{15,25} The absorption contribution from amorphous silicon is higher than that of crystalline silicon. Therefore, the region around 1100 nm is related to a transition region, where absorption is due primarily to the amorphous silicon and MR structures. During thermal annealing, the spike geometry does not change, but the amorphous silicon should be re-crystallized, which produces the observed absorbance decrease near 1100 nm.

IV. CONCLUSION

In conclusion, we designed and fabricated a high-aspect-ratio “black silicon” material, and experimentally demonstrated that the resulting surface structures can enhance the absorbance to >90% for a wide spectral range of 200–2500 nm. Importantly, by combining the MR structure and the phosphor-doped low impedance silicon, this high absorbance will not be affected by the high temperature processes associated with semiconductor device fabrication, especially in the infrared region. These results are meaningful for the eventual practical fabrication of semiconductor devices, such as infrared sensors, which need high absorbance and annealing-insensitive silicon.

ACKNOWLEDGMENTS

Thanks for the valuable suggestions from XuGuang Guo (Shanghai Institute of Microsystem and information technology).

This work was partly supported by the National Program on Key Basic Research Project of China (973 Program, 2012CB934203), “Chen Guang” Project of

Shanghai Municipal Education Commission and Educational Development Foundation (12CG54), State Scholarship Fund (201308310172), National Natural Science Foundation of China (11104186).

- ¹T. Her, R. J. Finlay, C. Wu, S. Deliwala, and E. Mazur, *Appl. Phys. Lett.* **73**, 1673 (1998).
- ²R. Younkun, J. E. Carey, E. Mazur, J. A. Levinson, and C. M. Friend, *J. Appl. Phys.* **93**, 2626 (2003).
- ³Y. Ma, H. Ren, J. Si, X. Sun, H. Shi, T. Chen, F. Chen, and X. Hou, *Appl. Surf. Sci.* **261**, 722 (2012).
- ⁴C. B. Simmons, A. J. Akey, J. J. Krich, J. T. Sullivan, D. Recht, M. J. Aziz, and T. Buonassisi, *J. Appl. Phys.* **114**, 243514 (2013).
- ⁵K. N. Nguyen, P. Basset, F. Marty, Y. Leprince-Wang, and T. Bourouina, *J. Appl. Phys.* **113**, 194903 (2013).
- ⁶J. de Wild, A. Meijerink, J. K. Rath, W. G. J. H. M. van Sark, and R. E. I. Schropp, *Energy Environ. Sci.* **4**, 4835 (2011).
- ⁷T. Chen, J. H. Si, X. Hou, S. Kanehira, K. Miura, and K. Hirao, *J. Appl. Phys.* **110**, 073106 (2011).
- ⁸H. M. Branz, V. E. Yost, S. Ward, K. M. Jones, B. To, and P. Stradins, *Appl. Phys. Lett.* **94**, 231121 (2009).
- ⁹H. K. Raut, V. A. Ganesh, A. S. Nairb, and S. Ramakrishna, *Energy Environ. Sci.* **4**, 3779 (2011).
- ¹⁰H. Nakanishi, S. Fujiwara, K. Takayama, I. Kawayama, H. Murakami, and M. Tonouchi, *Appl. Phys. Express* **5**, 112301 (2012).
- ¹¹P. Hoyer, M. Theuer, R. Beigang, and E.-B. Kley, *Appl. Phys. Lett.* **93**, 091106 (2008).
- ¹²V. Zorba, E. Stratakis, M. Barberoglou, E. Spanakis, P. Tzanetakos, S. H. Anastasiadis, and C. Fotakis, *Adv. Mater.* **20**, 4049 (2008).
- ¹³T. Baldacchini, J. E. Carey, M. Zhou, and E. Mazur, *Langmuir* **22**, 4917 (2006).
- ¹⁴M. A. Sheehy, L. Winston, J. E. Carey, C. M. Friend, and E. Mazur, *Chem. Mater.* **17**, 3582 (2005).
- ¹⁵C. H. Crouch, J. E. Carey, M. Shen, E. Mazur, and F. Y. Genin, *Appl. Phys. A* **79**, 1635 (2004).
- ¹⁶R. Torres, V. Vervisch, M. Halbwx, T. Sarnet, P. Delaporte, M. Sentis, J. Ferreira, D. Barakel, S. Bastide, F. Torregrosa, H. Etienne, and L. Roux, *J. Optoelectron. Adv. Mater.* **12**, 621 (2010).
- ¹⁷T. G. Kim, J. M. Warrender, and M. J. Aziz, *Appl. Phys. Lett.* **88**, 241902 (2006).
- ¹⁸S. M. Sze and K. K. Ng, *Physics of Semiconductor Devices* (Wiley, Hoboken, NJ, 2007).
- ¹⁹M. J. Weber, *Handbook of Optical Materials* (CRC, NY, USA, 2003).
- ²⁰Y. Peng, M. Hong, Y. Zhou, D. Fang, X. Chen, B. Cai, and Y. Zhu, *Appl. Phys. Express* **6**, 051303 (2013).
- ²¹T. Sarnet, M. Halbwx, R. Torres, P. Delaporte, M. Sentis, S. Martinuzzi, V. Vervisch, F. Torregrosa, H. Etienne, L. Roux, and S. Bastide, *Proc. SPIE* **6881**, 688119 (2008).
- ²²Y. Peng, Y. Wen, D. Zhang, S. Luo, L. Chen, and Y. Zhu, *Appl. Opt.* **50**, 4765 (2011).
- ²³Y. Peng, D. Zhang, H. Chen, Y. Wen, S. Luo, L. Chen, and Y. Zhu, *Appl. Opt.* **51**, 635 (2012).
- ²⁴B. R. Tull, J. E. Carey, E. Mazur, J. P. McDonald, and S. M. Yaliso, *MRS Bull.* **31**, 626 (2006).
- ²⁵N. Ott, M. Nerdling, G. Müller, R. Brendel, and H. P. Strunk, *Phys. Status Solidi* **197**, 93 (2003).